

UNCLASSIFIED

406 424

AD

DEFENSE DOCUMENTATION CENTER

FOR

SCIENTIFIC AND TECHNICAL INFORMATION

CAMERON STATION, ALEXANDRIA, VIRGINIA



UNCLASSIFIED

406424

JPRS: 17,370

Scale - 3

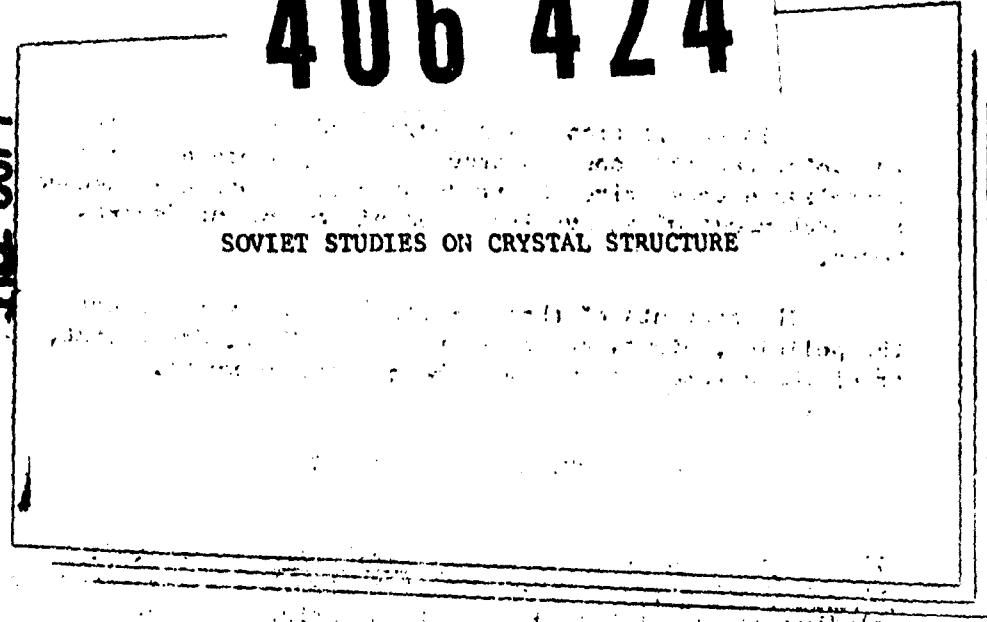
S&T

30 January 1963

406 424

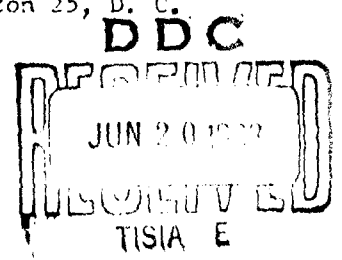
AD NO. _____

FILE COPY



U. S. DEPARTMENT OF COMMERCE
 OFFICE OF TECHNICAL SERVICES
 JOINT PUBLICATIONS RESEARCH SERVICE
 Building T-30
 Ohio Dr. and Independence Ave., S.W.
 Washington 25, D. C.

Price: \$1.00



NOTICE: When government or other drawings, specifications or other data are used for any purpose other than in connection with a definitely related government procurement operation, the U. S. Government thereby incurs no responsibility, nor any obligation whatsoever; and the fact that the Government may have formulated, furnished, or in any way supplied the said drawings, specifications, or other data is not to be regarded by implication or otherwise as in any manner licensing the holder or any other person or corporation, or conveying any rights or permission to manufacture, use or sell any patented invention that may in any way be related thereto.

FOREWORD

This publication was prepared under contract for the Joint Publications Research Service, an organization established to service the translation and foreign-language research needs of the various federal government departments.

The contents of this material in no way represent the policies, views, or attitudes of the U. S. Government, or of the parties to any distribution arrangements.

PROCUREMENT OF JPRS REPORTS

All JPRS reports are listed in Monthly Catalog of U. S. Government Publications, available for \$4.50 (\$6.00 foreign) per year (including an annual index) from the Superintendent of Documents, U. S. Government Printing Office, Washington 25, D. C.

Scientific and technical reports may be obtained from: Sales and Distribution Section, Office of Technical Services, Washington 25, D. C. These reports and their prices are listed in the Office of Technical Services semimonthly publication, Technical Translations, available at \$12.00 per year from the Superintendent of Documents, U. S. Government Printing Office, Washington 25, D. C.

Photocopies of any JPRS report are available (price upon request) from: Photoduplication Service, Library of Congress, Washington 25, D. C.

THE ROLE OF SEPARATION SURFACES IN THE
DELAYED FRACTURE OF METALS

Following is a translation of an article by I.A. Oding, V. S. Ivanova and Yu. P. Liberov in the Russian-language book Issledovaniya po zharoprochnym splavam (Research on Heat-Resistant Alloys) Vol 4, Publishing House of the Academy of Sciences USSR, Moscow, 1959, pages 3-12.

While developing the ideas of Greenwood [1], who first made use of the concept of vacant sites in the crystal lattice to explain the nature of delayed fracture of metal operating under pressure at high temperatures, Oding and Ivanova [2] have postulated that such defects have a role in the process of delayed fracture only if they possess the following characteristics:

1. The vacant sites arise from the plastic deformation of metals. Their number in tempered material is clearly inadequate to form even those pores and micro-fissures that are found in a metal long before its fracture. The movement of dislocations effecting plastic deformation brings about the formation of new vacancies.
2. The vacancies are mobile and their degree of mobility depends on the autodiffusion criteria of the metal [3].
3. The movement of vacant sites in a stressed metal is of a directional character and depends on the kind of stress: these vacancies are transformed from highly elongated to less elongated volumes and from these to compressed volumes. The rate of their directional displacement depends on the amount and gradient of stress (deformations) [2, 4].
4. Vacancies can coalesce, because two combined vacancies are thermodynamically more stable than two separated vacancies [5]. Hence vacancies can grow into large colonies and can form spaces and fissures of ultramicroscopic and microscopic dimensions, ultimately reaching values necessary [6] for the self-generated expansion of fissures.
5. Most favorable to the collection and deposition of vacancies are spaces of the metal which are situated at separation surfaces: the boundaries of grains and blocks, sliding surfaces, micropores, micro-fissures

and the boundary of twin crystals. Surfaces of secondary phases (aging phases), gaseous and non-metallic inclusions, are also considered as separation surfaces. The greatest gradients and degrees of strain are to be anticipated at all these sites and for this reason the accumulation and deposition of vacancies will be greatest here. If, for example, experimental conditions are such that plastic deformation is greatly affected by intergranular plasticity then the fracture of the metal will run along the grain boundaries. If deformation is due to intragranular plasticity with the formation of numerous shear surfaces and twins, then the fissures in the metal will grow within grains [2].

We emphasize that if the vacancies lack any one of these five properties then they cannot be used to explain fracture formation and development in the course of prolonged service under pressure at a high temperature. These properties have been hypothetically assigned to vacancies, hence we require experimental confirmation of the decisive role of vacancies in the delayed fracture of metals. We cannot, for example, consider that metal fracture due to accumulation of vacancies [7]. If the latter were merely movable and were unable to form colonies - to accumulate and be deposited at separation surfaces - and possessed no regular directionality in their displacement within a metal under stress, then they could not be assigned a significant role in the delayed fracture of the metal.

Evidently a metal's degree of saturation with vacancies is most accurately measured with dilatometrical and X-ray structure methods. For example, we can mention the following works: [8], in which the concentration of vacancies is measured with a dilatometer; [9], in which an X-ray structure method is used for this purpose, and [10] and [11] in which, respectively, calorimetry and density measurements were used. Measurement of electrical conductivity can lead to errors because this property is also predetermined by the density of dislocations which changes simultaneously with a change in the concentration of vacancies. Nevertheless, this method has also been used [12].

However all these methods are suitable for the macroscopic but not the microscopic evaluation of vacancy concentration. The use of a micro-hardness method likewise has its consequences, for the micro-hardness of a metal should rise with the accumulation of a number of single vacancies and be lowered by their coagulation; in this case we do not know to what extent an increased number of single vacancies is reflected in the change in micro-hardness and we also do not know the degree of coagulation of vacancies that produces a reduction in micro-hardness. In addition, with the prolonged use of heat-resistant metals under high temperatures and pressure, aging processes occur which more effectively change the properties of a metal in regions adjacent to separation surfaces in contrast to intragranular regions. Consequently in regions adjacent to separation surfaces the aging process advances

in time and depending on the degree of aging the micro-hardness can be greater than, less than or even equal to the micro-hardness of the metal in intragranular regions. In other words, the effects of aging with respect to magnitude and direction can conceal the effects of a change in micro-hardness due to displacement, coagulation and deposition of vacancies.

Finally, the change in the density of dislocations during the use of a metal under stress at high temperatures is very effectively reflected in a change of such properties as the micro-hardness and electrical conductivity [13]. Therefore the most acceptable method to detect the role of vacancies in the delayed fracture of a metal is for all intents and purposes the microscopic method, specifically that of electron microscopy, by means of which at even relatively small magnifications, of an order of 20,000 to 30,000x, it is possible to see colonies of vacancies with a diameter of 0.05-0.03 microns or 500-300 Angstrom units. Such investigations were performed by us on heat-resistant varieties of steel of mark EI 395, EI 257 and EI 432, samples of which were employed under creep conditions for several thousand hours. The widespread opinion that fissures propagate along grain boundaries only with prolonged use of a metal and that intragranular fracture occurs with short periods of use is frequently not justified although many have even related this postulate to the discontinuity of the dependence of long-term strength on time which is observed when this relationship is plotted on logarithmic coordinates. Thus, for example, as can be seen from the microphoto of the structure of austenitic steel EI 257 (fig. 1), which was subjected to a temperature of 575° and a stress of 20 kilograms/mm² for only 200 hours, the intergranular failure predominates in this case. Figure 2 shows a microphoto of austenitic steel EI 432 which was subjected to a temperature of 600° and stress of 18 kilograms/mm² for 4500 hours. In this case along with intergranular failure we also see evidences of marked intragranular deformation as well as intragranular fissures, demonstrating that the process of failure in internal regions of grains may occur in cases of prolonged use of the metal.

Hence it can be stated that intergranular or intragranular failure depend not only on testing conditions but also on the nature of the steel which determines the properties of the border and body of the grain. Both cases of failure, however, can be generalized into one: fissures form and grow at separation surfaces. We have not been able to detect a micro-fissure or a nucleus thereof outside of these regions. Intergranular micro-fissures are most frequently formed at junctions of three grains, which very strongly confirms the accuracy of Zener's theory [14], according to which delayed fracture of a metal occurs due to the relaxation of stresses at grain boundaries, which produces a quite effective concentration of stress in regions close to the junction of three grains. However this postulate of Zener's has no general significance.

It is enough to turn to figure 3, which shows a microphoto of EI 395 steel which has been employed for 9064 hours at a temperature of 575° and a pressure of $22 \text{ kilograms/mm}^2$, to show that along with the formation of fissure nuclei at junction sites of three grains micro-fissures are also formed at other sites.

How are micro-fissures formed and is the mechanism of their formation the same for separation surfaces of all kinds? Let us turn to the electron microphotos in figures 4, 5 and 6. These microphotos and those following were made on an EM-3 microscope with the use of colloid replica plating. Shading of the replicas was achieved by applying chromium to their surfaces. Interpretation of the electron microphotos revealed that the face of the slide was covered with cavities; only at isolated sites were inclusions found which projected onto the face of the slide. Figure 4 shows the boundary of two grains of EI 395 steel in their initial state. The boundary is quite clearly and cleanly outlined, without significant depositions of a secondary phase and without accumulated porosity.

The picture is markedly changed however following the use of the steel for 5519 hours at a temperature of 575° and pressure of $26 \text{ kilograms/mm}^2$ (figures 5 and 6). The clearness of the boundary is absent and the two grains are separated by a wide band (about 1 micron) consisting of an accumulation of small and large pores and rare secondary phase inclusions. The empty spaces, i.e. colonies of vacancies, vary in shape from rounded to quite elongated pores, blending into micro-fissures. The latter by growing acquire ever increasing dimensions and by branching out from not one but a network of fissures. In this process the width of the band and the character of porosity depend on the kind of steel. In comparing the microphotograph of figure 6 with that of figure 7 which shows at the same magnification the structure of the intergranular boundary of EI 257 steel after 7880 hours at a temperature of 575° and stress of $13 \text{ kilograms/mm}^2$, we can see that the width of the band is less and the colonies of vacancies are here considerably larger; and this demonstrates a greater degree of vacancy coagulation. The boundary of this band is cut sharply upon contact with the grain of the solid solution. A transitional zone of fragmented colonies of vacancies is lacking, which demonstrates the specificity of the process of vacancy deposition.

As analogous picture is also seen in the surface of twin crystals. Vacancy accumulation in this case is readily examined in the microphoto of EI 257 steel in figure 8 (test conditions were the same as for the metal presented in figure 7). Here twin boundaries have degenerated into fissures arising either from grain boundaries or from intragranular regions. These grains are also made up of vacancies located on the boundaries of twins (figure 9, EI 257 steel, test conditions identical to those for figures 5 and 6).

The role of such separation surfaces in the process of vacancy accumulation, as in the case of a sliding surface, is seen in figure 10, in which a microphoto of EI 432 steel is presented following 967 hours at a temperature of 600° and stress of 25 kilograms/mm². Clearly in evidence here are dislocations in the form of punctate formations lying in sliding surfaces and exposing one end onto the surface of the grain.

It is interesting to note one detail of grain boundary structure sometimes observed after prolonged use of a metal under creep conditions, -- a serrated structure at grain boundaries as is seen in figure 11, which pictures the microstructure of austenitic steel EI 257 after 11,250 hours under creep conditions at a temperature of 575°. The sample was under a stress of 11 kilograms/mm² for 5000 hours and was then loaded to 20 kilograms/mm². The dark lines (angles) that appeared apparently represent the accumulation of dislocations which migrated on the sliding surfaces from the body of the grain to its boundary (arrow a in fig. 11). The fields of force around such dense accumulations of dislocations create favorable conditions for the accumulation of vacancies, which also brings about the formation of fissure nuclei (arrow b in fig. 11).

With these findings we see a close relationship of the creep phenomenon with the process of delayed failure of metals. In Odling's work [15, 16] it is shown that the rate of creep is proportional to the density of dislocations developed for movement. This postulate has been experimentally confirmed [13, 20]. It was shown that with increased creep rate there is an increase in the hardness and electrical resistance of a metal, which can occur only with a considerable increase in the density of dislocations. It had seemed that with increased metal hardness there must be an increase in long-term stability and a decrease in the creep rate. However the large dislocation density increases the likelihood of temperature fluctuation effects, which brings about an increased creep rate. An increase in the density of dislocations also implements the deposition of vacancies in those areas of force fields that show signs of compression. Hence creeping at an increasing rate unavoidable brings about the failure of a metal although the stress in this case is considerably lower than those which bring about metal failure, for example, in the case of active tension.

Certain investigators [17-19] consider the process of delayed failure of metals as a process of reducing break resistance from the amount of the stress of external forces operating on the metal. Certainly a reduction in the profile of a sample due to the accumulation of empty spaces (colonies of vacancies) must bring about a change in the break resistance of a metal. But this is not the principal feature of delayed fracture. If this were limited only to a change in break resistance as is understood in the hardness testing of a metal, for example in stretching at continuously increasing tension, then the break in continuity must be

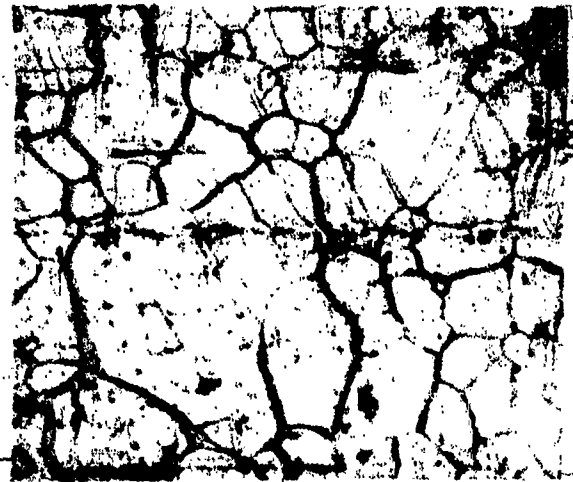


Fig. 1. Intergranular character of EI 257 steel failure after creep testing.
 $\sigma = 20 \text{ kg/mm}^2$; $T = 575^\circ$;
 $t = 200 \text{ hrs.}$

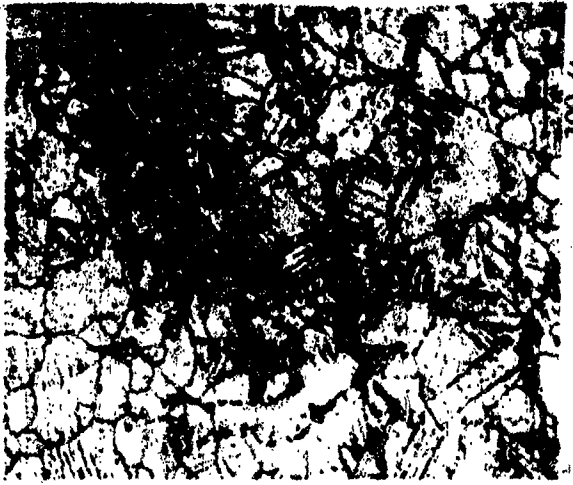


Fig. 2. Failure of EI 432 steel along sliding surfaces and grain boundaries after creep testing.
 $\sigma = 18 \text{ kg/mm}^2$; $T = 600^\circ$;
 $t = 4500 \text{ hrs.}$



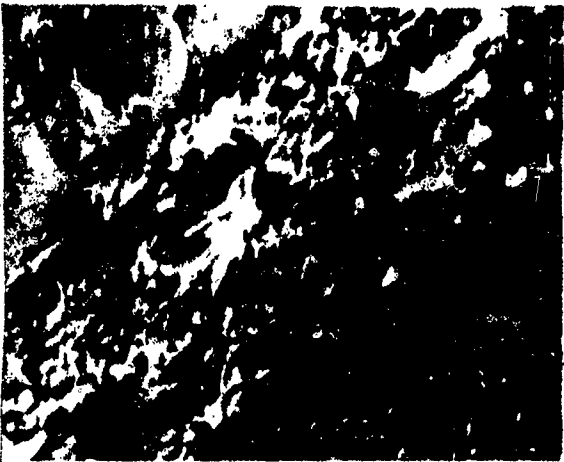
Fig. 3 Intergranular failure of EI 395 steel after creep testing.
 $\sigma = 22 \text{ kg/mm}^2$; $T = 575^\circ$;
 $t = 9064 \text{ hrs.}$



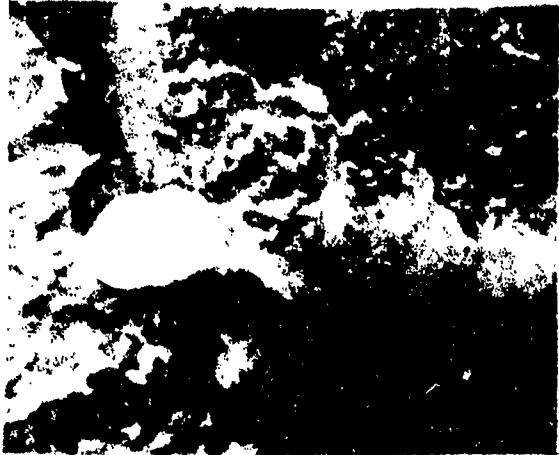
1.5μ
Fig. 4. Initial microstructure (electron microscope) of EI 395 steel



1.5μ
Fig. 5. Disintegration along grain boundaries (electron microscope) of EI 295 steel after creep testing.
 $\sigma = 26 \text{ kg/mm}^2$; $T = 575^\circ$; $t = 5519 \text{ hrs.}$



1.5μ
Fig. 6. Micro-fissures along grain boundaries (electron microscope) of EI 395 steel after creep testing.
 $\sigma = 26 \text{ kg/mm}^2$; $T = 575^\circ$; $t = 5519 \text{ hrs.}$



1.5 μ
 Fig. 7. Micro-fissures along grain boundaries (electron microscope) of EI 257 steel after creep testing.
 $\sigma = 18 \text{ kg/mm}^2$; $T = 575^\circ$;
 $t = 7880 \text{ hrs.}$



100 μ
 Fig. 8. Fissures along grain boundaries and twin boundaries in EI 257 steel after creep testing.
 $\sigma = 18 \text{ kg/mm}^2$; $T = 575^\circ$;
 $t = 7880 \text{ hrs.}$

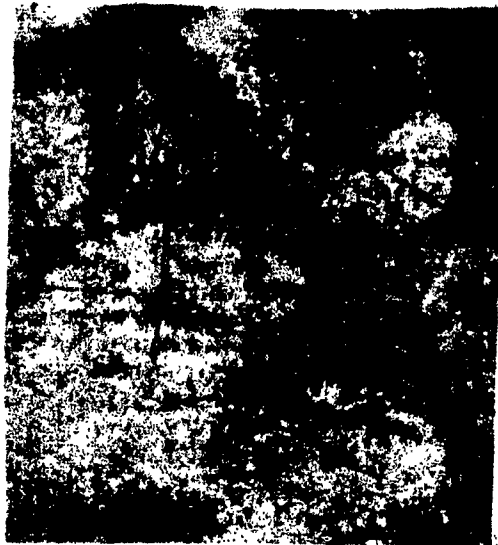


1.5 μ
 Fig. 9. Disintegration along twin boundaries (electron microscope) of EI 257 steel after creep testing.
 $\sigma = 26 \text{ kg/mm}^2$; $T = 575^\circ$;
 $t = 5519 \text{ hrs.}$



10 μ

Fig. 10. Vacancy accumulation along sliding surfaces in EI 432 steel after creep testing.
 $\sigma = 25 \text{ kg/mm}^2$; $T = 600^\circ$; $t = 967 \text{ hrs.}$



10 μ

Fig. 11. Vacancy accumulation along grain boundaries (optical microscope) of EI 257 steel after creep testing.
 $t = 11, 250 \text{ hrs.}$

developed instantaneously with the operating tension and must bring about fracture of the sample. In creep tests this comes about only at the last moments of the test, when fissures have grown to dimensions that satisfy the conditions of Griffith for self-generating expansion of fissures. In delayed fracture the fissure nuclei appear long before the final break. Hence if delayed fracture of metals is to be viewed only as a process of changing break-resistance characteristics then it becomes unclear why the first break in continuity does not occur at once upon loading of the sample, but only tens, hundreds and thousands of hours later, and after having appeared, develops again over a long period of time.

Only processes of a diffusional character that require some time for their development can explain the processes of delayed fracture in metals. In this respect the application of the theory of vacant sites in the crystal lattice has been completely substantiated. This theory also explains the role of separation surfaces in the process of delayed fracture. Grain and block boundaries as well as sliding surfaces and twin boundaries, being sites of the greatest dislocation density, because of the presence of fields of force about the dislocations attract vacancies to themselves which migrate due to autodiffusion throughout the entire volume of the grain. Fields of force also implement the deposition of vacancies in those volumes which are experiencing compression stresses. The formation of stable colonies of vacancies must be looked upon as the first and most essential step of delayed fracture: groups of vacancies become sedentary and other migrant vacancies by settling out at the surfaces of these colonies are combined with them. One must not expect a significant concentration of vacancies in a relatively thick layer of metal around a separation surface, for an increased concentration of migrating vacancies can be local only in the ultramicroscopic sense. This is why in the electron microphotographs presented above there is no transitional zone: the boundary strip generated by colonies of vacancies is abruptly cut upon contiguity with the solid solution. Finally, even the fact that nuclei of discontinuities at grain boundaries are frequently observed at the junction sites of three grains can also be explained by the theory of vacancies in the crystal lattice, for in these junctions the elastic deformation of the latter must be at its greatest, and consequently the conditions for vacancy deposition are improved.

CONCLUSIONS

This analysis of the microstructure of certain heat-resistant varieties of steel which were subjected for a long period of time to stress at high temperatures affirms that the most probable mechanism of the delayed fracture of metals is the process of vacancy formation and deposition.

Of course, with employment of an alloy the precipitation and coagulation of secondary phases can also bring about substantial deterioration of corresponding regions of the parent solid solution and grain boundaries. However these processes can play a significant role only when the alloy is employed under conditions which do not assure the adequate stability of its structure. With adequate stability of the alloy the main role in the process of delayed fracture can only be ascribed to vacancies. In this process separation surfaces play an exceptionally great role, attracting vacancies to compressed regions of a force field set up around an imperfection in the crystal lattice.

BIBLIOGRAPHY

1. J. N. Greenwood, J. Iron and Steel Inst., Vol 171, page 380, 1952.
2. I. A. Oding, V. S. Ivanova, DAN SSSR (Doklady Akademii Nauk SSSR - Reports of the Academy of Sciences USSR), Vol 103, No 1, 1955.
3. Ya. I. Frenkel', Vvedeniye v teoriyu metallov (Introduction to the Theory of Metals), 1950.
4. C. Crussard, J. Friedel, Symposium on Creep and Fracture of Metals at High Temperatures, May 31 to June 2, 1954.
5. F. Seitz, Advances in Physics, Vol 1, No 1, 1952.
6. A. A. Griffith, Phyl. Trans. Roy. Soc. Vol 221, page 163, 1921.
7. I. L. Mirkin, I. I. Trunin, in the collection: Ispytaniye i svoystva zharoprochnykh materialov (Testing and Properties of Heat-resistant Materials), pages 25-44, 1957.
8. J. Blean, C. R., 237, 1953.
9. J. Blean, A. Guinier, C. R., 236, 1953.
10. Clarebrough and others, Proc. Roy. Soc. A. Vol 215, page 507, 1952.
11. Clarebrough and others, Philos. Mag. Vol 1, No 6, pages 528-536, 1956.
12. T. H. Blewit, R. R. Colman, J. K. Redman, "Work Hardening in Copper Crystals," Report of the Conference on Defects in Crystalline Solids, University of Bristol, pages 369-382, 1954.
13. I. A. Oding, V. S. Ivanova, Issledovaniya po zharoprochnym splavam, (Research on Heat-resistant Alloys), Vol 3, Academy of Sciences USSR Publishing House, 1958.
14. C. Zener, Fracturing of Metals, American Society for Metals, 1958.
15. I. A. Oding, Issledovaniya po zharoprochnym splavam, Vol 2, 1957.
16. I. A. Oding, DAN SSSR, Vol 116, No 1, 1957.
17. S. T. Kishkin, DAN SSSR, Vol 95, No 4, 1954.
18. S. T. Kishkin, Metallovedeniye i obrabotka metallov (Metalworking and the Processing of Metals), Vol 12, 1957.
19. Ya. B. Fridman, B. A. Drozdovskiy, DAN SSSR, Vol 95, No 4, 1954.
20. V. S. Ivanova, L. K. Gardiyenko, Metallovedeniye i obrabotka metallov, Vol 6, 1958.

5888

CSO: 1879-D

EFFECT OF CRYSTAL STRUCTURE DEFECTS ON CERTAIN
PROPERTIES OF METALS AND ALLOYS

Following is a translation of an article by I. Ya. Dakhtyar, V. S. Mikhalenkov and E. G. Madatova in the Russian-language book Issledovaniya po zharko-prochnym splavam (Research on Heat-Resistant Alloys), Vol. 4, Publishing House of the Academy of Sciences USSR, Moscow, 1959, pages 71-77.

We know that the properties of real metals are determined by the nature and character of the distribution of imperfections present in them [1]. Efforts of investigators in recent years have been directed to the study of the properties of various sorts of imperfection in metals, such as: vacancies, dislocated atoms, impurities of foreign atoms and dislocations. As a result of these studies it has been established that the physico-mechanical properties of metals are conditioned not only by the movement of various defects of the crystalline lattice but also by the nature of their interaction.

A study of the different properties of metals with respect to their structural make-up may provide useful information not only of the nature of the effect of defects in the lattice on properties of the metals but also on the mechanisms of various processes. Present findings now indicate, for example, that the effect of plastic deformation on electrical resistance of metals can be explained by the formation and interaction of vacancies, dislocated atoms and dislocations. In precisely the same manner the increase in the diffusion coefficient during plastic deformation can be explained by the increase in the concentration of vacancies with deformation and the character of their interaction with defects of dislocation [2]. On the other hand we know of many data which indicate that under certain conditions the movement of various defects conditions the deformation observed in the metal. With this we can apparently explain the deformation of thin wires of a diameter equal to that of the grain, which is discussed in reference [3], as well as viscous sliding along grain boundaries [4]. The interaction of vacancies with dislocations can also explain the movement of signs observed in the Kirkendahl effect [5].

These phenomena allow us to express the following hypothesis. If the external force applied to a metallic object produces stress and deformation effecting a change of state of any defects present in it, then conversely the interaction of the defects and their change of state and distribution may be the result of the deformation of the sample

Plastic Deformation During Repeated Hardening

One of the manifestations of this relationship is the deformation discussed below of polycrystalline metallic shapes due to their repeated hardening. If a metallic sample is subjected to frequent cooling from a high temperature or to repeated cycles of heating and cooling correspondingly higher and lower than the temperature for polymorphic transformation, then it is deformed, being stretched out in one direction and shortened in another [See Note].

[Note]: The phenomenon was observed in the works of A. A. Bochvar, B. G. Lazarev as well as Ye. I. Ivanov and their coworkers.

In research performed up to the present workers have been concerned with samples of metals or alloys complex in their form and content and although important relationships have been detected, the mechanism of the phenomenon remains undiscovered.

In order to study the mechanism of this phenomenon we have striven to maximally simplify the conditions of the experiment. The experiment was conducted with samples in the form of thin wires or foils. The diameter of the samples was varied from 0.5 to 0.9 mm and the length from 140 to 150 mm. Test objects were pure metals (99.99%): silver, gold and certain alloys ([Note]: Samples of gold, -brass and Cu-Au alloy had a width of 4 mm and thickness of 0.1 mm.) Before treatment with the thermocycles the samples were annealed at a temperature higher than the corresponding maximal hardening temperature. In this process the dimensions of the crystals approximately corresponded with the diameter of the sample.

Preliminary testing with silver showed that at a constant hardening temperature the elongation of the thin sample was proportional to the number of thermocycles as a first approximation. Graphs of the

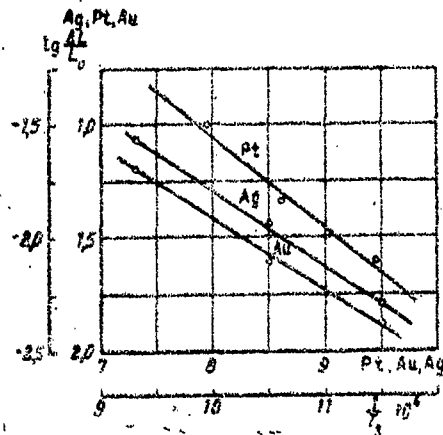


Fig. 1. Relationship of $\lg \frac{\Delta L}{L_0}$ to $\frac{1}{T}$ for platinum, gold and silver.

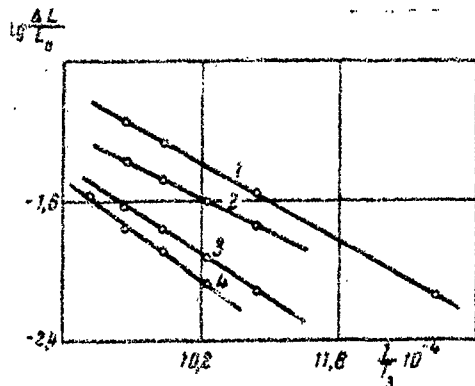


Fig. 2. Relationship of $\lg \frac{\Delta L}{L_0}$ to $\frac{1}{T}$ for alloys.
 1- α and β brass;
 2 - α -brass;
 3- Cu-Au foil;
 4- Cu-Au wire.

temperature relationship of the deformation $\frac{\Delta L}{L_0}$ for the test objects are presented in figures 1 and 2. Plotted on the abscissa are the values of $\frac{1}{T}$ where T is the hardening temperature, and on the ordinate $\lg \frac{\Delta L}{L_0}$ in which L_0 is the initial length of the sample. All changes in deformation are related to a constant number of thermocycles. The path of these curves satisfies the relationship

$$\epsilon = \frac{\Delta L}{L_0} = A \exp\left(-\frac{U}{kT_s}\right), \quad (1)$$

in which A and U are certain constants depending on the material.

Assuming that microscopic deformation is conditioned by an excessive concentration of vacancies ($\Delta n_s \approx n_s = N \exp\left(-\frac{U}{kT_s}\right)$) obtained after each hardening and by the character of their movement due to interactions with dislocations, then we can write that

$$\frac{\Delta L}{L_0} = A' \nu N \exp\left(-\frac{U_s}{kT_s}\right), \quad (2)$$

in which N is the number of atoms in 1 cm³, and U_B is the energy of vacancy formation. The data presented in table 1 show that the calculated values of U, determined according to formula (1), approximate the values of U_B, the energy of vacancy formation.

In order to explain the direction of deformation the authors resort to the dislocation mechanism of deformation.

It is asserted that vacancies are most easily generated at dislocations [7]. These are not only the sources but also the outlets

Table 1

Metal	A, $\frac{\text{mm}}{\text{mm}}$	U, $\frac{\text{kcal}}{\text{mol}}$	U _B , $\frac{\text{kcal}}{\text{mol}}$	n _j	N _d , cm ⁻²
Silver.....	0,6·10 ⁸	18,3	15,9 [8]	6·10 ⁸	6·10 ¹¹
Gold.....	1,23·10 ⁸	16,2	16,4 [8]	4,7·10 ⁸	4,7·10 ¹¹
Platinum.....	2,75·10 ⁸	23,0	27,2 [8]	2,0·10 ⁸	2,0·10 ¹¹
Platinum & 10%rhodium..	1,1·10 ⁸	21,6	—	5,2·10 ⁸	5,2·10 ¹¹
-brass.....	0,875·10 ⁸	10,8	8,0 [11]	7,5·10 ⁸	7,5·10 ¹¹
& -brass.....	0,534·10 ⁸	12,4	—	10,5·10 ⁸	1·10 ¹²
Cuzau foil.....	0,55·10 ⁸	15,1	—	9,34·10 ⁸	0,9·10 ¹²
Cuzau wire.....	0,53·10 ⁸	16,0	—	9,7·10 ⁸	1,0·10 ¹²

for the vacancies. Stresses occur in hardening which in the case of thin wires are greater radially than along the axis of the sample. These stresses are due to the appearance of new dislocations, i.e., additional outlets for the vacancies.

Stresses can be reduced due to the annihilation of vacancies with dislocations, which occurs at the next heating period after the hardening. In the case of wires of a diameter approximately equal to

the caliber of the grain, excessive vacancies due to the reduction of stress can escape on the crystal surface. But this must be compensated for by a movement of atoms in the opposite direction, as a result of which the sample is stretched out on its axis and reduced in cross section.

If by n_j we designate the number of dislocation points per unit length of the dislocation which are outlets for excess vacancies, then the elementary deformation thereby brought about can be expressed in the following manner [8]:

$$\epsilon = \frac{b^2}{n_j} \Delta n, \quad (3)$$

where b is Burgers' vector. By juxtaposition we obtain:

$$\frac{\Delta L}{L_0} = \frac{v b^2 N}{n_j} \exp\left(-\frac{U_b}{kT_s}\right) \quad (4)$$

By juxtaposing formulas (1) and (4) we have:

$$A \approx \frac{v b^2 N}{n_j} \quad (4a)$$

According to reference [7] the average number of dislocation points per unit length of dislocation which cause dislocation is:

$$n_j = f N_d \quad (5)$$

in which f is a coefficient less than one that designates the effective number of points serving as outlets for vacancies; ℓ is the length of free run of a dislocation, and N_d is their density.

From formulas (4a) and (5) it is possible to estimate the density of dislocations:

$$N_d \approx \frac{v b^2 N}{f A} \quad (6)$$

if we make an assumption as to the value of the free run path $\sim \ell$ (half the distance from the origin of the dislocation to the barrier). If d is the distance between active sliding surfaces then the average distance between dislocations will be $(\ell d)^2$. This distance has a value of the order $\sim 10^{-4}$ cm. Then $\ell d = 10^{-8}$ cm². From the data of electron microscopy, the distance between active sliding surfaces is of the order of 100-1000 Å. Hence $\ell \approx 10^{-3}$ cm, and the dislocation

density of 10^{11} cm^{-2} (table 1) estimated from these data corresponds adequately with the estimate from other methods.

Effect of Plastic Deformation on Diffusion Rate of Nickel Alloys

An important question, which elucidates the interaction of various defects of the crystal structure, is the effect of plastic deformation at elevated temperatures on the mobility of atoms in metals and alloys [2]. This question has scarcely been studied, although its study would aid in elucidating the mechanism of plastic deformation of metals at high temperatures.

For this experiment [2] we developed and built a vacuum apparatus within which during the annealing process an axial load of constant value is applied to the sample surface to which a diffusing substance has been applied (usually a radio-isotope of some metal).

The samples are cylinders with plane-parallel bases, 1.5 mm high and 7.5 to 12 mm in diameter, in order to produce different pressures at one and the same load. The samples are separated by molybdenum packings and thin annealed mica foils. The latter perform two functions: 1) they exclude the diffusion of atoms of the radio-active indicator that covers the sample surface into the molybdenum packing; and 2) they serve as lubricants to reduce friction between the facings of the samples and the packing. The set up makes it possible to obtain pressures up to 10 kilograms/mm² and temperatures up to 1200°C, which are regulated by a thermoregulator with an accuracy of 2°.

With this set up we studied the dependence of diffusion rate into nickel alloys with molybdenum on the rate of deformation at elevated temperatures. Diffusion coefficients were determined by using the radio-active isotope Co^{60} , a thin layer of which was electrolytically applied to the sample surface by the absorption method. This method makes use of the γ -radio-activity of the sample before and after diffusion annealing.

The diffusion rate $\dot{\epsilon}$, which for not very long periods of deformation can be considered as almost independent of time, is determined by the formula:

$$\dot{\epsilon} = \frac{l}{t},$$

in which mean deformation is

$$\dot{\epsilon} = 2 \ln \frac{R_t}{R_0}$$

Figure 3 graphs the relationship of diffusion rate on deformation rate for Ni-Mo alloys with a molybdenum content of 6.53, 9.57 and 16.68 at. % at a temperature of 1050°C.

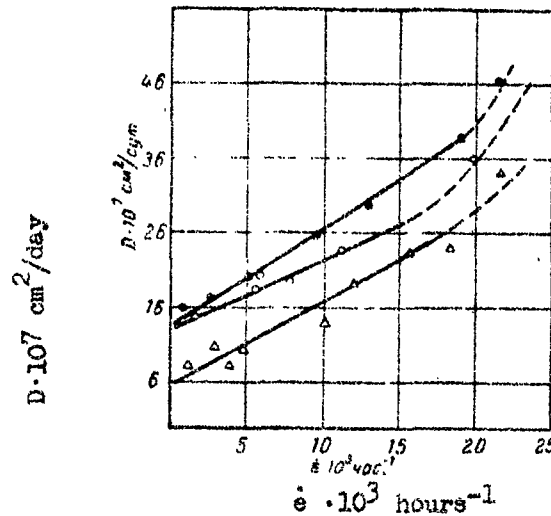


Fig. 3. Relationship of diffusion rate to deformation rate for alloys of the Ni-Mo system ($t = 1050^\circ$) with molybdenum content (at. %):

• - 6.53; ○ - 9.57; △ - 16.68.

The data obtained indicate that at small deformation rates the diffusion is proportional to the rate of deformation (at constant temperature), while at larger deformation rates the diffusion rate increases more rapidly and non-linearly with respect to the deformation rate.

The first condition can be grasped by examining the following interaction of vacancies with dislocations [9].

1. Vacancies can deposit out at dislocation sites or leave them.
2. In order to displace a linear dislocation perpendicular to a sliding surface it is necessary to displace mass, which can be achieved by the diffusion of vacancies to the dislocations.
3. At thermal equilibrium atoms arrive at the site with the same frequency. If the concentration of vacancies in the material surrounding the dislocation exceeds the equilibrium value then the

rate of arrival of vacancies at the site increases. Accordingly an excess of vacancies is the moving force for displacement of a dislocation in a direction perpendicular to the sliding surface.

During deformation vacancies can arise as a result of the migration of corresponding dislocation sites and be annihilated at the outlets, most frequently in places where dislocations are dense. Under these conditions at a stationary state the rate of vacancy formation in any elementary volume is equal to the rate of their annihilation. This leads to the establishment of a gradient of concentration for vacancies in a layer at some depth from the surface, approximately equal to

$$\Delta x \approx 2\sqrt{D_v T^*},$$

where D_v is the diffusion coefficient of a vacancy, and T^* is its lifetime in a zone of constant vacancy concentration [7].

The rate of vacancy generation (number/cm³/sec.) according to references [7, 8] is

$$R_g = \frac{n_d \dot{\epsilon}}{b^2}, \quad (7-8)$$

in which n_d is the average number of sites per unit length of dislocations which form vacancies, $\dot{\epsilon}$ is the deformation rate, and b is Burgers' vector.

In order that during deformation the diffusion rate is always in excess it is necessary to maintain the gradient of vacancy concentration at the depth Δx . But for this condition the rate of vacancy generation at some area ΔS perpendicular to the direction of diffusion must be equal to the flow of vacancies discharged through that area. Only thus can an excessive diffusion coefficient ΔD be maintained stationary in time, brought about by an increased concentration of vacancies in this area. This conditions can be expressed in the following manner:

$$\frac{n_d \dot{\epsilon} \Delta x}{b^2} = D_v \frac{\Delta c}{\Delta x}, \quad (9)$$

in which Δc is the excess of vacancies per unit volume (as compared to their equilibrium number at a given temperature) in the layer Δx .

Let N be the number of atoms per cm³, then the increase in the diffusion coefficient in this layer is

$$\Delta D = \frac{\Delta c}{N} D_v = \frac{n_d \dot{\epsilon}}{N b^2} (2\sqrt{D_v T^*})^2. \quad (10)$$

If m is the average number of vacancy leaps between a source and an outlet, then

$$D_v T^* = mb^2. \quad (10a)$$

For high temperatures \overline{m} ,

$$m = \frac{1}{\alpha' N_d n_d b^2}, \quad (11)$$

in which α' is a coefficient characterizing the effectiveness of annihilation of vacancies with a dislocation site.

If v is the energy of the reaction between a vacancy and a dislocation, then

$$\alpha' \approx 1 - \exp\left(-\frac{v}{kT}\right). \quad (11a)$$

By solving expressions (10), (10a) and (11) for the diffusion coefficient during plastic deformation we obtain:

$$D_v = D_{v=0} + \Delta D = D_{v=0} + \frac{4}{N \alpha' N_d b^2} \dot{\epsilon}. \quad (12)$$

This expression indicates that the rate of softening $\frac{d D_f}{d \dot{\epsilon}}$ increases with a decrease in the dislocation density due to the fact that the probability of blocking them is diminished.

With a linear relationship of the diffusion coefficient on the rate of deformation it is possible to estimate the density of dislocations (table 2); here it is assumed that $\alpha' \sim 1$, and $b = 2 \cdot 10^{-8}$ cm.

Table 2

Mo, wt. %	6,53	9,57	16,25
N_d cm ⁻² (950°)	$1,3 \cdot 10^8$	$2,8 \cdot 10^8$	$1,8 \cdot 10^8$
N_d cm ⁻² (1050°)	$1,0 \cdot 10^8$	$1,58 \cdot 10^8$	$1,21 \cdot 10^8$
N_d cm ⁻² (1150°)	$0,8 \cdot 10^8$	$0,9 \cdot 10^8$	$0,87 \cdot 10^8$

The comparatively small density of dislocations shown in table 2 apparently indicates that under these conditions of deformation at high temperatures crowded dislocations occur.

With formula (12) it is possible to calculate the density of dislocations from data on the effect of axial pressure upon the rate of auto-diffusion of α -iron [10]. At 890° it turns out that $D_{\sigma} = D_{\sigma=0} \cdot (1 + 50 \dot{\epsilon})$, in which $\dot{\epsilon}$ is expressed in hours⁻¹. At 890° $D_{\sigma=0} = 4.3 \cdot 10^{-11}$ cm²/sec., whence, by assuming $\dot{\epsilon} \approx 1$, we obtain:

$$N_d = 7.4 \cdot 10^6 \text{ cm}^{-2}.$$

Thus the data obtained for the effect of plastic deformation on the diffusion process confirm the hypothesis that the displacement of dislocation type defects underlies the mechanism of plastic deformation at high temperatures.

BIBLIOGRAPHY

1. I. Ya. Dekhtyar, Uspekhi fizicheskikh nauk (Advances in the Physical Sciences) Vol 62, page 99, 1957;
Voprosy fiziki metallov i metallovedeniya (Problems in the Physics of Metals and Metal Working). Academy of Sciences of the Ukrainian SSR, Vol 7, page 53, 1956.
2. I. Ya. Dekhtyar, V. S. Mikhalukov, Information Brief, INF, Academy of Sciences, Ukrainian SSR, Vol 8, 1957;
Tezisy dekladov na XI nauchno-tekhnicheskoy sessii po zharoprotivnyam splavam (Thesis Reports at the 9th Scientific-Technical Session on Heat-resistant Metals), Moscow, 1957.
3. C. Herring, J. appl. Phys., Vol 21, page 437, 1950.
4. N. F. Nabarro, Proc. Bristol Conf. on Strength of Solids, Vol 75, 1958.
5. A. D. Denler, Uspekhi fiziki metallov (Advances in the Physics of Metals), Vol 1, page 224, 1956.
6. S. D. Gertsiken, DAN SSSR, Vol 48, No 2, 1954.
7. F. Seitz, Acta met., Vol 1, page 355, 1953.
8. E. S. Macklin, J. Metals, Sect. 2, Vol 8, page 106, 1956.
9. T. Kead, "Dislocation in Crystals", II, 1957.
10. F. Suffington, K. Cohen, J. Metals, Vol 4, No 8, 1952.
11. E. Gerin, K. Elleckson, J. Chem. Phys., Vol 9, page 742, 1941.

-558
 DRG: 1373-D

EXPERIMENTAL OBSERVATION OF SOURCES OF DISLOCATIONS
ON THE BASIS OF SEPARATIONS

Following is a translation of an article by V. G. Rakin and N. N. Buynov in the Russian-language book Issledovaniya Po Zharoproschnym Splavam (Research on Heat-Resistant Alloys), Vol 4, Publishing House of the Academy of Sciences USSR, Moscow, 1959, pages 193-196.

According to the scheme proposed by Frank and Read [1], new dislocations can be generated by a source in the form of almost circular closed loops, however up to the present the sources of dislocations have not been discovered. Only Wilsdorf and Kuhlmann-Wilsdorf [2], on observing groups of little chains of separations in an alloy of aluminum with several percent copper in the electron microscope, proposed that each group of separation chains was formed at dislocations generated by a source.

On examination with electron microscopy of a Al-Cu alloy (4% Cu) aged at 190° for 4 hours and at 250° for 30 minutes, we detected chains of separations in the form of nearly closed continuous or broken loops, close in form to a circle (fig. 1). Apparently these loops are produced as a result of the formation and growth of separations at dislocations generated by a source. The closer the orientation of a surface [Note]: Surface orientation is determined by the orientation of the separations is to a plane of type (111), the more complete and distinct the loops appear (fig. 1), and the number observed is greater. However the loops or rings are also detected on other planes (fig. 1, b). For example of 43 photographs with sources examined, in 8 cases the orientation of the plane in which the source was located was approximately (111), in 10 cases it was (112), in 6 cases it was (122), in 7 cases it was (123), and the orientation approximated (100) and (110) in 2 cases. The orientation could not be determined in 8 cases. The loops are seen best on plane (111), then on (112) and (122), worse on (123), and very poorly on planes close to (110) and (100).

The possibility of observing loops of dislocation along separations in planes other than (111) is partly due to the large diameter of θ' -phase plates being separated at the dislocations (from 0.1 to 0.25 μ).

microns). Then too in certain cases an error could occur in the determination of surface orientation, for, due to deformation that occurs in an alloy on hardening, separations of two orientations have principally been observed; a third orientations has been encountered only rarely. The possibility of an error has been increased by the small dimensions of particles of separations in the matrix beyond the area encompassed by dislocation loops, as a result of which accurate determination of the orientation of separations was excluded.

The loops almost always had a "center" like the opening of a hexagon or other shape (fig. 1, b; fig. 2). In some cases an

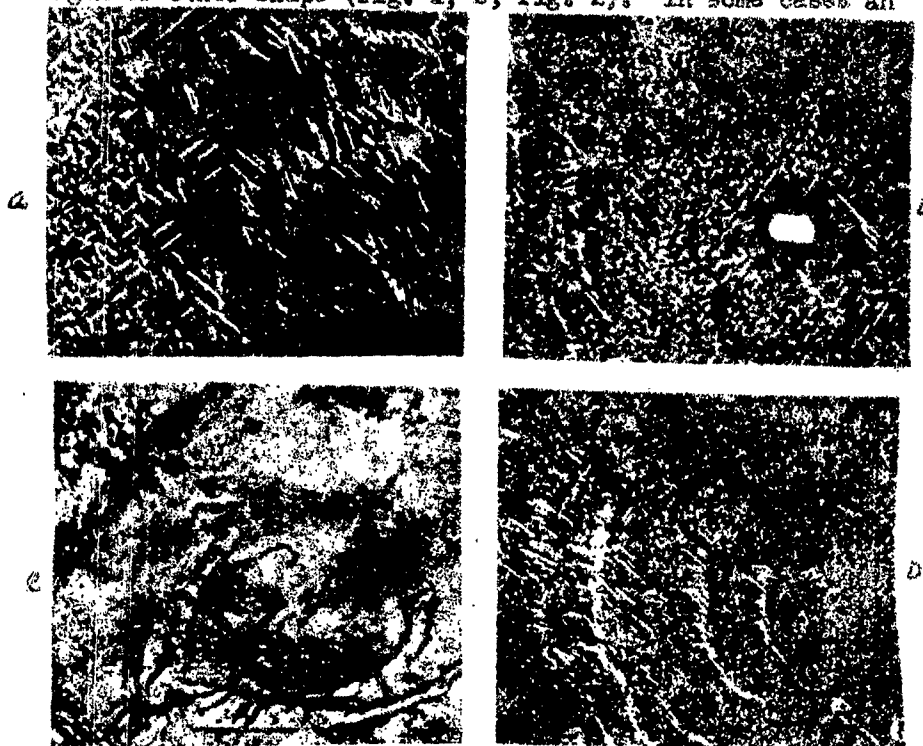


Fig. 1. Separation chains in Al-Cu alloy: a-aging at 190° for 4 hours (20,000X); b- aging at 190° for 4 hours (15,000X); c- aging at 250° for 30 minutes, etched with aqua regia (15,000X); d- aging at 190° for 4 hours (15,000X).

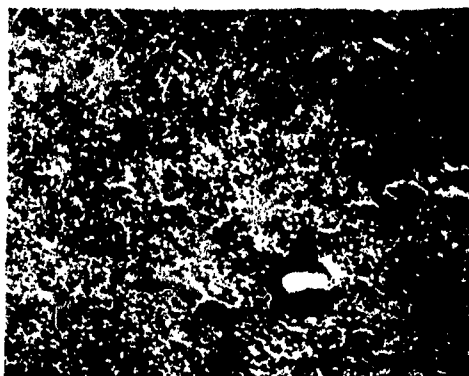


Fig. 2. Al-Cu alloy; aged at 190° for 4 hours (15,000X).

inclusion or an irregular etching figure was observed in the center. At the present time the nature of these "centers" has not been established. In most cases with remoteness of loops from the "center" the distance between loops is somewhat increased. An evaluation from 17 measurements indicated that if the average distance of the first loop from the center is 0.47 microns, then between the first and second and the third and fourth loops it is 0.55 and 0.72 microns respectively, and between loops most remote from the source it reaches 1.75 microns.

Complete confirmation has not been given to the hypothesis of Wilsdorf and Kuhlmann-Wilsdorf [3] to the effect that laminate separations at dislocations must have only one orientation, namely such that the line of their intersection with the distribution surface of the dislocation forms the least angle with the axial direction of the latter. Although the separations at dislocations principally had one orientation, nevertheless in almost all cases at some segments of a loop separations of two and sometimes even three orientations were observed. The angle between the axis of dislocation and the line of intersection of separation particles with the surface in which the dislocation lies was $20-30^{\circ}$, but deviations to one side or the other were frequently observed. In replicas obtained from electrically polished samples the loops formed by the separations were incomplete in most cases. This can be explained in two ways. First, by the fact that the dislocation loop consists of individual links which appear as marginal and spiral dislocations, the possible orientation of which is shown by the arrows in fig. 1,c, and respectively designated by the letters K and B. Second, by the fact that, in accordance with reference [3], separations in Al-Cu alloys are formed only at marginal dislocations (in our case at marginal links of a loop). If the links making up the loop and the distance between separations are correspondingly small, then the loop is continuous; if these links have a size of several tenths of a micron then it will appear to consist of individual fragments.

The existence of separations of predominantly one orientation along the entire length of the loop (fig. 1,a) indicates that the latter actually is made up of links of marginal and spiral dislocations and that all the marginal components have a single orientation. In order to ascertain the structure of the loops a portion of the samples after electropolishing was deeply etched in aqua regia following which oxide replicas of them were taken. As is evident from photos of the samples, the loops are far more deeply etched than the segments between and beyond them, (fig. 1,c) but almost always they appear to be incomplete. Accordingly the dislocation loop apparently consists of segments which appear to be marginal and spiral dislocations.

According to dislocation theory, the minimal dislocation stress τ , necessary for activation of a Frank-Read source of length l , of an emitting dislocation with a burgers vector of b , is given by the expression:

$$\tau = \frac{Gb}{l}$$

in which G is the module of the displacement.

The length of the source l can be estimated from measurements of the "center". From the photographs taken with 26 measurements the linear size of the "center" was equal to 0.4 microns. If b is taken as 2.8 Angstroms and G as 2700 kg/mm², then τ is 1.9 kg/mm², which approximately corresponds to the yield point of the alloy. Consequently our measurements of the sources can be considered as accurate.

In addition to those in figure 1, sometimes (about one case in ten) sources of another type are observed which produce two ellipsoidal loops extending into opposite sides with an interrupted distribution of separations along them (fig. 2). This apparently is explained by the fact that the "center" can contain two dislocations of opposite sign, the ends of which are so securely fixed that they cannot be approximated and mutually annihilated although they also experience mutual attraction. Upon application of external stress both dislocation lines begin to generate dislocation loops of different sign.

We have estimated the density of dislocation sources in the surfaces corresponding to or close to planes (111) or (122), (112) and (123). In the mean of ten measurements, the source density was $5 \cdot 10^5 \text{ cm}^{-2}$, whereas in some works it has been reported as from 10^8 cm^{-2} ^[4] to 10^9 cm^{-2} ^[5]. From one sample replicas were obtained at different depths from the surface (250, 500 and 800 microns). The metal layers were removed from the surface by electropolishing. Sources of dislocations were seen in all of these cases, but their density varied, corresponding to $4 \cdot 10^5$ to $8 \cdot 10^5$ and $2 \cdot 10^5$ to $3 \cdot 10^5 \text{ cm}^{-2}$. The number of dislocation loops about each source was observed as from 2 to 10, but on the average (from 75 photographs) it was from 3 to 5.

Thus these experiments provide yet another confirmation to the dislocation theory of separations.

BIBLIOGRAPHY

1. F. C. Frank, W. T. Read: Phys. Rev., Vol 79, page 722, 1950.
2. H. Wilsdorf, D. Kuhlmann-Wilsdorf, Phil. Mag. Vol 45, No 369, page 1096, 1954.
3. H. Wilsdorf, D. Kuhlmann-Wilsdorf, Report of the Conference on Defects in Crystalline Solids, London, 1955, pages 175-186.
4. N. F. Mott, Phil. Mag., Vol 43, No 346, page 1151, 1952.
5. D. Kuhlmann-Wilsdorf; J. H. van der merwe, and H. Wilsdorf, Phil. Mag., Vol 43, No 341, page 632, 1952.

5888
CSO: 1879-D

STUDY OF SUBMICROSCOPIC DEFECTS IN METALS BY THE METHOD
OF X-RAY BEAM SCATTERING AT LOW ANGLES

Following is a translation of an article by S. N. Zhurkov and A. I. Slutsker in the Russian-language book Issledovaniya Po Zharoprochnym Splavam (Research on Heat-Resistant Alloys), Vol 4, Publishing House of the Academy of Sciences USSR, Moscow, 1959, pages 197-201.

As we study the actual structure of metals more and more heterogeneity is encountered in their structure. The image of the ideal crystal lattice and its fundamental properties which has been such a great achievement of the physics of solids is because of research being constantly supplemented with new departures from the ideal structure. Now it has been firmly established that the ideal crystal structure is disrupted by thermal oscillations of atoms, vacancies, atoms, intrusions into interstices, impurities, block structure, dislocations and the like.

Of the many types of defects encountered in the crystal lattice of metals, our work will concern itself with heterogeneities characterized by variation in electron density, which is frequently equivalent to ordinary density irregularities. Such irregularities may be empty spaces (fissures, pores), precipitated phase regions in alloys during dispersion hardening, amorphous intercalations at grain boundaries, strongly stressed blocks, dislocation disruptions, etc.

Heterogeneities of this type can be of great interest, for example, the presence of submicroscopic fissures causes a significant difference in theoretical and practical yield strength, temperature-endurance effects on strength, creep, and the like. On the other hand, dispersion precipitated phases markedly alter the properties of a metal, increasing its mechanical characteristics in comparison to the solid solution.

One means of studying irregularities in electron density is a method based on x-ray beam scattering at small angles, the physical basis for which is as follows.

If a thin pencil of x-rays is passed through a layer of a substance having electron density irregularities with dimensions of an order of 10 to 1000 wavelengths of a given x-ray source then a halo will appear close to the primary beam -- a scatter that falls off rapidly with increase in the angle (fig. 1).

Dispersion theory makes it possible to use the angular function of a scattered beam and its intensity to calculate the dimensions of heterogeneities, their concentration, and in the most favorable cases -- their shape and orientation. In the simplest case of non-densely packed, monodisperse, spherical irregularities, diffuse scattering close to a thin primary beam is quite accurately determined by the formula:

$$I = N(n - n_0)^2 e^{-\frac{4\pi^2 R^2 \sin^2 \varphi}{\lambda^2}} \quad (1)$$

In which I is the intensity of a beam with wavelength λ , scattered at angle φ , expressed in units of single electron scatter; R and N are the radius and number of spherical irregularities taking part in the scatter, and n and n_0 are the number of electrons in the region of heterogeneity and in an equal volume of its surroundings.



Fig. 1. X-ray scatter close to the primary beam.

Note that since formula (1) involves the square of the difference of the electron densities at the region of heterogeneity and its environs, scatter will occur at a positive or negative value of this difference, including particles in an empty space as well as pores in a continuous medium. In this way measurements of the angular spread of x-ray scatter intensity at small angles permits us to obtain detailed information on defects in metals and alloys of interest to us.

Unfortunately, in spite of its great potential, this method has not attained widespread use, evidently due to ignorance of it as well as certain difficulties in experimentation with it and in the interpretation of the results obtained. In experimental study of the small angle scatter of x-rays by submicroscopic heterogeneities two basic difficulties arise:

1. In the majority of cases the scatter comprises a very small share of the incident beam ($I/I_0 \approx 10^{-5}$ to 10^{-7}).

2. Appreciable scatter lies in a region of very small angles with respect to the axis of the primary beam, sharply falling off with an increase of the angle (θ). At wavelengths of the order of 1 Angstrom unit the region of appreciable scatter for particles with linear dimensions R lies up to

$$\begin{aligned} 3^\circ & \text{ when } R \approx 10 \text{ \AA} \\ 20' & \text{ when } R \approx 100 \text{ \AA} \\ 2' & \text{ when } R \approx 1000 \text{ \AA} \end{aligned}$$

The requirement of measuring a weak scattered ray at such small angles close to the powerful primary beam is quite a difficult experimental task.

The problem with most of the instrumentation described in the literature is their small light intensity and the considerable background which increases rapidly with decrease in the angle. Superimposed on a weak scatter emission this background makes the instrument unsuited for the study of defects in pure metals and in many cases even in alloys.

Below is described a variation of the slit method which greatly eliminates these problems. The apparatus which is outlined in figure 2 has been developed to measure scatter at ultrasmall angles and has been quite effective in the study of the submicroscopic structure of substances producing weak scatter.

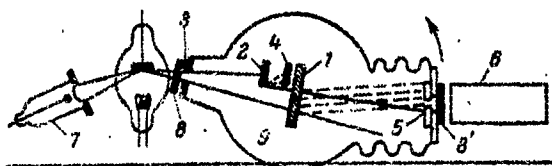


Fig. 2. An apparatus for measuring scatter at ultrasmall angles.

A thin plate of the test sample (1) is exposed to a wide divergent x-ray beam with a sharp border created by a lead gate (2) whose edge has been well polished. Sharpness of the border in this case is determined by the width of the entry slit (3) and the geometry of the device. Rays scattered by the edge of the gate (2) are collected by a lead foil (4) which is set by control screws at the very border

of the primary beam. The angular dispersion of the beam scattered by the sample (1) is measured by the slit (5) which together with an end-type Geiger-Mueller counter or a photomultiplier scintillation counter (6) is rotated in the plane of the figure around an axis passing through the sample. The x-ray source is the URS-55 with BSVL type tubes. Instability of the x-ray tube was corrected by a second counter (7), and the necessary monochromaticity of the scatter recorded was achieved by optimal operation of the tube, suitable filters (8) and (8'), optimal thickness of the test sample and the selectivity of the gas counter or by the discriminator during scintillation recording. In order to exclude scatter in the air of the slit, the gates and the sample were enclosed in a vacuum reservoir (9).

The use of a wide beam considerably increased the light intensity of the device and the use of a gate with a foil in place of a slit sharply reduced background and made it possible to come up to the edge of the primary beam at ultrasmall angles measuring fractions of a minute. In addition, the use of ionization recording instead of photography, due to a marked increase in sensitivity, makes it possible in the differential method of measurement to exclude residual background and to obtain the desired values for the amount of scatter at small and ultrasmall angles.

The operation and rating of the device were tested on standard objects — dilute aqueous solutions of globular proteins of known molecular size. Measurements demonstrated a satisfactory correspondence of the dimensions and concentration of protein molecules obtained by the method of small angle scatter with results of other tests.

The apparatus provides for the introduction into the vacuum chamber of equipment to study metals in the process of deformation at various temperature and testing conditions.

Figure 3 shows data on the measurement of small angle scatter (measurements performed at a wavelength of 1.5 \AA , background has been subtracted in all the graphs) in thin foils of sheet metals (Al, Zn, Ni, Ag, Pt). The presence of a uniform discrete angular dependence of scatter intensity in the region of small angles demonstrates the existence in these metals of defects 200 to 500 \AA in size.

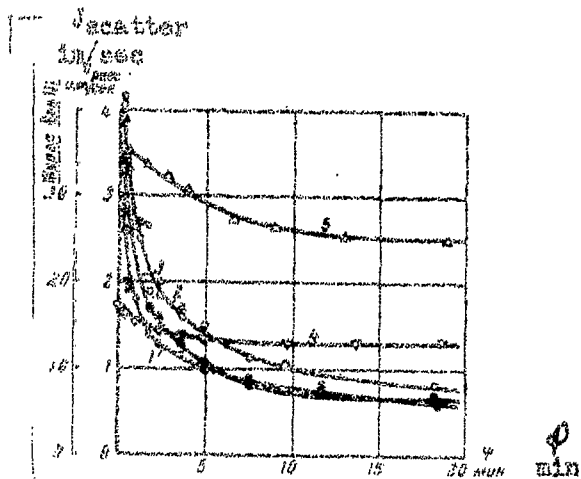


Fig. 3. Small angle scatter in thin foils of pure sheet metals: 1-Al, 80 microns; 2-Zn, 35 microns; 3-Ag, 12 microns; 4-Pt, 12 microns; 5-Ni, 23 microns.

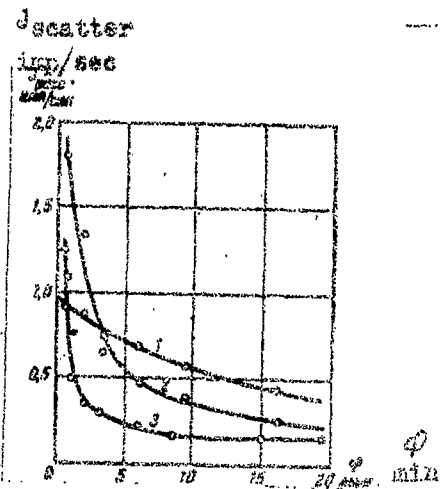


Fig. 4. Small angle scatter in aluminum: 1-sheet; 2-annealed in vacuum (640° , 5 hrs.); 3-monocrystalline, obtained by annealing recrystallization.

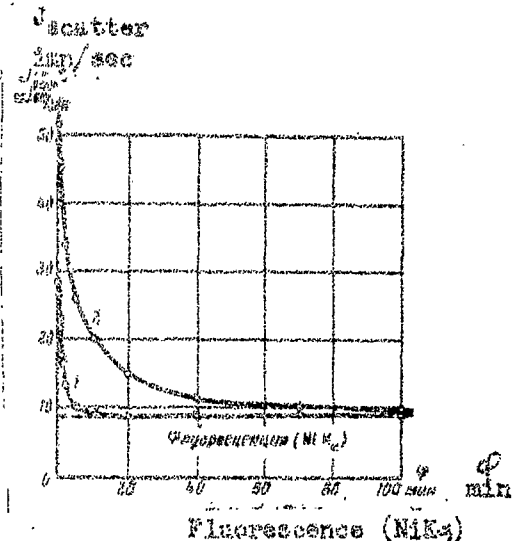


Fig. 5. Small angle scatter in nickel 50 microns thick: 1-initially (annealed); 2-deformed by tension in which $\sigma = 23 \text{ kg/mm}^2$.

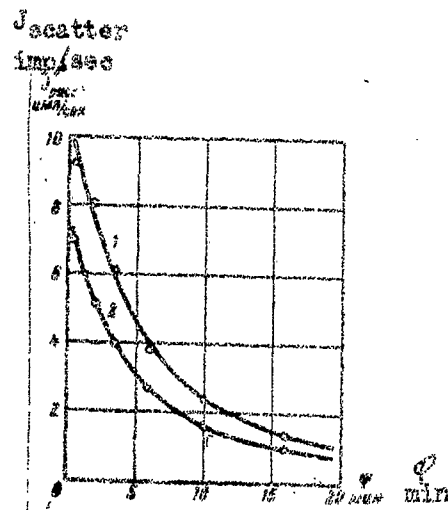


Fig. 6. Scatter intensity in aluminum: 1-deformed by tension; 2-after electropolishing.

The irregularities in structure do not disappear even after prolonged high-temperature annealing in a vacuum. Upon annealing aluminum sheet up to a temperature of 640° there occurs a decrease in the number and an increase in the size of the defects, which follows from the increase in the slope of the curves in figure 4. It is interesting to see that submicroscopic defects also occur in monocrystalline aluminum obtained by annealing recrystallization (curve 3 in figure 4).

Figure 5 presents data on the change in scatter with deformation of annealed nickel. From the graph it is evident that the principal scatter changes occur at very small angles. If scatter determinations were limited to angles of a degree and more then it is possible to arrive at a false conclusion of the absence of defects in the initial state of the material as well as to arrive at reduced values for their size.

The density change ($\Delta\rho/\rho \approx 10^{-5}$), calculated from our measurements on the assumption that these defects are empty spaces, corresponds well with direct measurements of the density reduction of the deformed aluminum.

This result as well as the high stability of the irregularities during intensive annealing make it quite likely that these defects are empty spaces or fissures in the metal.

These investigations have also established that the greatest change in submicroporosity occurs at an early stage of metal deformation, corresponding to the first portion of a creep curve. Somewhat later anisotropy of the scattered beam occurs, demonstrating the non-spherical shape of the defects and a certain orientation in their position. The defects must obviously be considered as disc-shaped with their plane perpendicular to the tension axis. Further, small angle scatter indicates that the vacancies arising from deformation are unequally distributed in the volume of the sample. The removal by electropolishing of a superficial layer several microns thick reduces scatter intensity out of proportion to the thickness of the layer removed (fig. 6), which indicates an increased (by 2 to 3 times) concentration of fissures in the surface layer.

The method of small angle x-ray scatter can be applied to the study of dispersion deposits at early stages in alloys and also makes it possible to detect submicroscopic defects and to investigate their behavior.

5888
OSO: 1879-D

- END -